Ultrafast detection of charged photocarriers in conjugated polymers

Daniel Moses, Arthur Dogariu, and Alan J. Heeger
Institute for Polymers and Organic Solids, University of California, Santa Barbara, Santa Barbara, California 93106
(Received 2 September 1999)

Ultrafast measurements of transient excited-state absorption in the spectral region spanning the infrared-active vibrational active (IRAV) modes in the prototypical luminescent polymers, poly(phenylene vinylene) (PPV) and poly[2-methoxy-5-(2-ethyl-hexyloxy)-(phenylene vinylene)] (MEH-PPV), reveal charge carrier generation within 100 fs after photoexcitation. The photocarrier quantum efficiency in MEH-PPV is $\phi_0 \approx 0.1$ in zero applied electric field. There is no correlation between the temporal behavior of the photoinduced IRAV signals and the exciton lifetime. Thus, carriers are photoexcited directly and not generated via a secondary process from exciton annihilation. Comparison of the recombination dynamics in MEH-PPV and PPV demonstrates the importance of the strength of interchain interaction on the carrier recombination dynamics. The quantum efficiency is the same ($\phi_0 \approx 0.1$) when the system is pumped either at photon energies well above the first π-π^* transition (at 267 nm, 4.7 eV) or when pumped into the first π-π^* transition (at 400 nm, 3.1 eV). The carrier lifetime, however, increases at the higher photon energy, providing a natural explanation for the increase in the photoconductivity at photon pump energies above 3 eV.

INTRODUCTION

Although the onset of steady-state photoconductivity coincides with the onset of absorption in PPV and its soluble derivatives, it has been known for some time that there is a large increase in the magnitude of the photoconductive response at higher energies (typically above approximately 3 eV). Chandross *et al.*[1] used the separation between the onset of absorption and the onset of this higher energy photoconductive response to infer an exciton binding energy of approximately 1 eV. More recently, Köhler *et al.*[2] presented an experimental study of the steady-state photoconductivity action spectrum coordinated with quantum chemical calculations of the wave functions of higher lying excited states in a model oligomer [i.e., states at energies above the lowest ($1B_u$) excited state]. They noted two points:

(1) Their measurements showed that when C_{60} is added in quantities of approximately 1:1 per polymer repeat unit, the magnitude of the sensitized photoconductivity[3] near the onset of the lowest π-π^* transition becomes comparable to that observed in the pure polymer at photon energies above 3 eV.

(2) Quantum chemical calculations for the model oligomer showed that there are higher lying excited states (at $\sim$5.6 eV) in which there is a higher probability of finding the electron and hole separated by a few phenyl rings. These states correspond to excitations polarized in the plane of the π network with strong contributions perpendicular to the chain axis. The more ''delocalized'' character of these higher excited states (with higher probability of intrachain spatial separation between the electron and hole than in the $1B_u$ state) was identified as being of principal importance. Their model is based on the comparison of these calculations with the photoconductivity action spectra of MEH-PPV and heavily doped MEH-PPV/C_{60} composites; both systems exhibit an increase of the photocurrent at photon energies above 3 eV.

Quite generally, however, photoconductivity is proportional to the product of $N_c \mu \tau$, where N_c is the density of photoinduced charge carriers, μ is the mobility, and τ is the carrier lifetime.[3] Note that $N_c = \phi_0 n_{\mathrm{ph}}$ where ϕ_0 is the quantum efficiency (QE) for photogeneration of charge carriers, $n_{\mathrm{ph}} = I\alpha/h\nu$, I is the incident flux of the pump beam (intensity/cm^2), α is the absorption coefficient of the pump beam, and $h\nu$ is the photon energy. Thus, in order to deduce N_c, one needs to know the detailed behavior of τ and μ at various photon energies. Moreover, N_c, μ, and τ are all time dependent. Thus, steady-state photoconductivity measurements such as those reported by Köhler *et al.*[2] are inherently difficult to interpret.

We have utilized an approach for directly measuring the density of photoinduced charge carriers in semiconductor polymers at subpicosecond times (100 fs temporal resolution).[4] This is accomplished by transient photoinduced absorption (PIA) measurements, pumped in the visible and probed in the 6–10 μm spectral region which spans the infrared active vibrational (IRAV) modes in conjugated polymers. This approach opens a unique window to the carrier generation process since it directly probes the carrier density. Once N_c is known, the mobility in the subnanosecond regime (and its dependence on temperature, external field, etc.) can be determined from the photoconductivity.

When introduced onto the backbone of a conjugated polymer either by chemical doping or photoexcitation, charged carriers (solitons, polarons, or bipolarons) break the local symmetry and thereby transform the even parity Raman-active vibrational modes into odd-parity infrared-active modes (IR vibrational modes).[5,6] Consequently, the IRAV modes are distinguished from the ''normal'' IR-active modes by being in 1:1 correspondence with the strongest Raman-active modes of the polymer backbone, as observed in resonant Raman scattering.[5,6] Because the IRAV modes are turned on by local charges, the strength of the IRAV absorption provides a probe for the carrier density generated either by chemical doping or photoexcitation.

On the contrary, since neutral bound states of an electron and a hole have zero net charge at any point, photogeneration of neutral excitons do not lead to photoinduced IRAV modes. Indeed, as discussed in the next section, there is clear experimental evidence that neutral excitons do not contribute to the IRAV signals.

Using transient, photoinduced IRAV mode absorption measurements, pumped in the visible and probed with 100 fs temporal resolution, we demonstrate a relatively large quantum efficiency for photogeneration of charged carriers in MEH-PPV, $\phi_0 \approx 0.1$. Although the initial quantum efficiencies for charge generation are approximately the same in PPV and MEH-PPV, the carrier decay rate is much faster in MEH-PPV, implying that τ is sensitive to the strength of the interchain coupling. We find that the initial density of photogenerated carriers is insensitive to the pump energy; the quantum efficiency is the same ($\phi_0 \approx 0.1$) when the system is pumped either at photon energies well above the first π-π^* transition (at 267 nm, 4.7 eV) or when pumped into the first π-π^* transition (at 400 nm, 3.1 eV). The carrier lifetime, however, increases at the higher photon energy.

These findings indicate that charged carriers (positive and negative polarons) are primary photoexcitations, and suggest a simpler alternative explanation for the increase in the photoconductivity at high photon energies: From the point of view of a conjugated chain in a higher excited state, neighboring chains appear as ''acceptors.'' The situation is similar to the photoinduced electron transfer from a conjugated chain in the first excited state to a nearby C_{60} molecule[7,8] In this case, however, the specific conjugated chain excited to a higher level acts as a ''super-donor'' to the neighboring chains. As a result, ultrafast interchain charge transfer is significantly enhanced at high photon energies, leading to longer carrier lifetime and thereby to the observed increase in the photoconductivity above 3 eV in PPV and its soluble derivatives.[1,2] Thus, while the onset of enhanced photoconductivity above 3 eV has a natural explanation in terms of reduced carrier recombination because of interchain charge separation, the onset of the photogeneration of charge carriers coincides with the onset of the lowest π-π^* interband absorption.

Finally, we note that the observation of photoinduced IRAV at 100 fs after photoexcitation confirms the ultrafast formation of polarons predicted nearly 20 years ago by Su and Schrieffer.[9]

PHOTO-INDUCED IRAV MODE MEASUREMENTS: A DIRECT, ALL-OPTICAL, ULTRAFAST PROBE OF THE CHARGE CARRIER DENSITY

The utilization of photoinduced IRAV modes for measuring photocarrier density was reported by Mizrahi *et al.* for MEH-PPV/C_{60}.[10] With a temporal resolution on the order of 100 ps, they demonstrated PIA with the spectral signatures of the IRAV modes, identical to those observed in steady-state experiments. We have extended this initial work by probing the photocarrier density via PIA measurements in the IRAV spectral region with significantly higher temporal resolution (100 fs), by measuring the photoinduced IRAV signals in pristine samples of PPV and MEH-PPV, and by determining ϕ_0 from the ratio of the signals obtained in pristine MEH-PPV and the MEH-PPV/C_{60} composite.[4]

In doped conjugated polymers, the strength of the IRAV modes is proportional to the doping level. Upon photoexcitation of pure semiconducting polymers,[11] there is a one-to-one correspondence between the photoinduced IRAV modes (steady-state and transient) and the doping-induced IRAV modes of the same polymers.[6,9,11] Thus, the strength of the photoinduced IRAV modes is directly proportional to the density of photogenerated charge carriers on the polymer chain. These experimental observations in conjunction with the detailed theoretical work of Horovitz and others[5,6] have established the mechanism by which charged carriers generate the IRAV modes.

Based upon this detailed theoretical understanding of the origin of the IRAV modes, one concludes that neutral excitons do not generate IRAV absorption because electron-hole bound states have zero net charge everywhere. Experimental results are consistent with this observation. In MEH-PPV, for example, we find that the lifetime of the photoinduced IRAV modes and the exciton lifetime are different; the IRAV lifetime is more than an order of magnitude shorter than the lifetime of the neutral excitons as inferred from the photoluminescence decay time.[7]

When mixed with acceptors such as C_{60}, conjugated polymers (e.g., PPV, MEH-PPV, etc.) undergo ultrafast photoinduced electron transfer with an associated increase in the PIA (both, steady-state and transient)[7] and the photoconductivity[8] signals, and with an associated decrease in the photoluminescence.[7] As expected for photoinduced electron transfer, the strength of the photoinduced IRAV modes is proportional to the concentration of C_{60} in polymer/C_{60} composites. These observations provide direct experimental evidence that neutral excitons do not generate IRAV mode absorption. If excitons did generate IRAV mode absorption, addition of C_{60} would reduce the strength of the photoinduced IRAV modes, since the exciton density is quenched by efficient photoinduced electron transfer. In contrast, a significant increase in the IRAV mode PIA signal is measured upon addition of C_{60}.

We conclude that the strength of the photoinduced IRAV mode absorption provides a direct, all-optical, ultrafast probe to the charge carrier density at the short-time scales ($t < 100$ fs) typical of carrier thermalization in disordered semiconductors.

PHOTOINDUCED IRAV MEASUREMENTS: DETAILS OF THE EXPERIMENTAL METHOD

An amplified Ti-sapphire laser system, equipped with an optical parametric amplifier (OPA), was used to produce 100 fs pulses at a repetition rate of 1 KHz. The modified Spectra Physics OPA system (shown in Fig. 1), pumped by the amplified oscillator at ω_{pump}, generates idler and signal beams with photon frequencies ω_i and ω_s, where $\omega_{\text{pump}} = \omega_i + \omega_s$. These two beams were mixed in a nonlinear crystal ($AgGaSe_2$) to generate a beam at $\omega_{\text{probe}} = \omega_s - \omega_i$,[12] tuned to the desired probe beam frequency ω_{IRAV} in the 6–10 μm range. The probe pulse bandwidth was approximately 0.02 eV, consistent with that expected from the Fourier transform of the short pulses. For the pump beam, we used the fundamental laser beam at 800 nm, its second harmonic at 400 nm,

and its third harmonic at 267 nm.

The probe pulse was tuned to the IRAV frequencies as determined by Mizrahi *et al.*[10] for MEH-PPV/C_{60}. Although the intrinsic bandwidth of the 100 fs pulses ($\Delta\lambda \sim 1$ μm, for λ between 6 and 10 μm) prevented accurate determination of the IRAV spectrum, the PIA signals resulted from photoinduced enhancement of the IRAV bands; see Ref. 10 (to resolve the sharp features in the IRAV spectrum requires pulse widths >1 ps). In our experiments, PIA was detected only when ω_{probe} was tuned to the IRAV modes (around 7 and 9 μm); there was no detectable signal when probed in the IR but well away from the IRAV modes (e.g., at wavelengths shorter than 5 μm).

Measurements were taken on free-standing (15 μm thick) stretched-aligned PPV (draw ratio of $1/1_0 = 4$), on films of MEH-PPV (40 μm thick) and on two MEH-PPV/C_{60} blends (10% and 50% C_{60} by weight with thickness of 2 and 12 μm, respectively). The MEH-PPV and MEH-PPV/C_{60} films were prepared by drop-casting onto KBr substrates. In order to produce more homogeneous MEH-PPV/C_{60} blends, we used the soluble derivative of C_{60}, 1-(3-methoxycarbonyl)propyl-1-phenyl[6,6]C_{61}.

DETERMINATION OF THE QUANTUM EFFICIENCY FOR PHOTOGENERATION OF CHARGE CARRIERS

Photoinduced IRAV mode absorption in MEH-PPV/C_{60} confirms charge transfer in less than 100 fs. Ultrafast electron transfer from the photogenerated excited state of PPV (and its soluble derivatives) to C_{60} occurs because the lowest energy unoccupied state in C_{60} lies within the energy gap and because energy can be conserved in the charge-transfer process by promoting the hole left behind to a higher energy state within the relatively broad π band of the semiconducting polymer.[13] Because of the ultrafast charge transfer, the quantum efficiency (QE) for charge separation and charge carrier generation in MEH-PPV/C_{60} approaches unity, consistent with the quenching of the photoluminescence[7,8] and the enhancement of the photoconductivity in blends containing C_{60}.[8]

Thus, the QE for photogeneration of charge carriers in the semiconducting polymer can be determined from the ratio of the photoinduced IRAV signals from MEH-PPV and MEH-PPV/C_{60}. Additionally, by comparing the photoinduced IRAV signals in PPV (where there are no side chains) and MEH-PPV (where the side chains introduced for improved solubility reduce the strength of the interchain hopping interaction), we demonstrate the sensitivity of the rate of carrier recombination to the strength of interchain interactions.

In stretch-aligned PPV samples, the photoinduced infrared absorption (in the IRAV spectral range) is polarized along the chain axis as expected for photoinduced IRAV modes. Because of the complete absorption of light polarized perpendicular to the orientation axis in the thick PPV samples (15 μm thickness), the photoinduced IRAV absorption is independent of the polarization of the pump beam.

When pumped at 800 nm, the dependence of the PIA signal strength on light intensity (I) in stretched aligned PPV is quadratic, as shown in the inset of Fig. 2. Since the excitation is via two-photon absorption, the I^2 dependence of the PIA indicates a linear dependence of the PIA signal on the carrier density.

Figure 2 shows the PIA wave form as obtained from PPV when excited at 800 nm and probed at 7 μm. The PIA response is limited by the system temporal resolution, $\sim$100 fs. Figure 3 depicts the PIA risetime in PPV, where the solid curve represents a step function convoluted with a Gaussian with 100 fs full width at half maximum. A fast initial PIA decay due to mono- and bimolecular recombination (identified from the variation of the PIA wave form at various I) is followed by a longer-lived exponential decay with $\tau = 250$ ps. While the PIA decay rate might be expected to increase at higher I (due to bimolecular recombination at high carrier densities), the peak photoinduced IRAV signal observed in our experiments is linear with I.

Figure 4 compares the photoinduced IRAV signal obtained from MEH-PPV to that obtained from MEH-PPV/C_{60} (50% C_{60}, by weight) when pumped with identical intensity at 800 nm and probed at 7 μm. Similarly, Fig. 5 compares

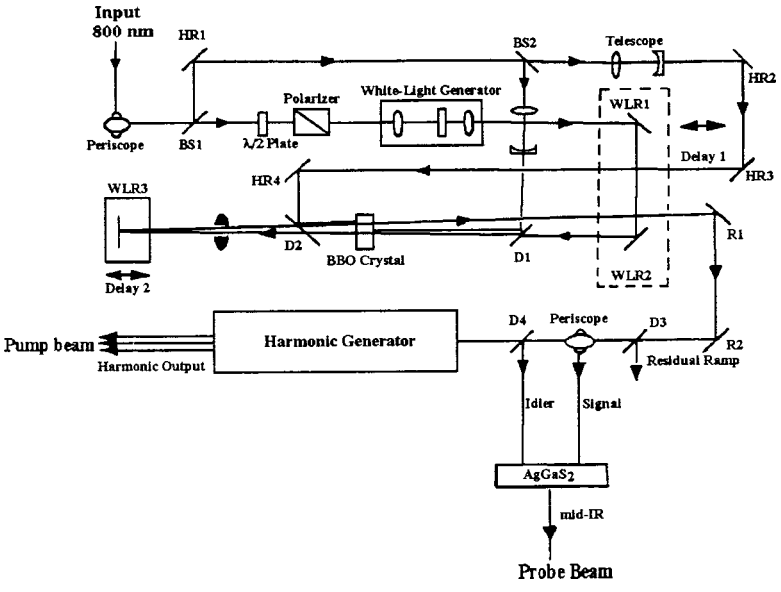

FIG. 1. Schematic diagram of the modified Spectra Physics OPA system used for generating the pump and probe beams for the photoinduced IRAV measurements; the output of an amplified Ti-sapphire laser (at 800 nm) serves as the input to the OPA; $AgGaS_2$ is the difference-frequency mixing crystal used for generating the probe beam; the harmonic generator unit prepares the harmonics of the signal or idler beams, to be used as the pump beam; BS 1,2 are beam splitters; HR 1–4 are high reflectors for 800 nm, WLR 1–3 are white-light reflectors; *D* 1–4 are dichroic mirrors; *R* 1,2 are output reflectors.

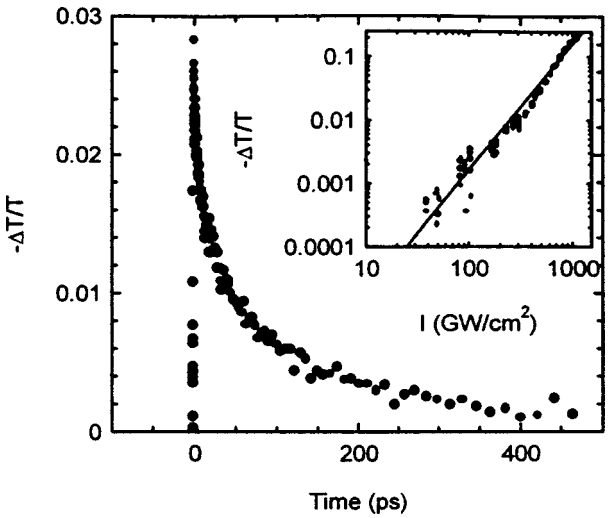

FIG. 2. The measured PIA wave form in PPV when pumped at 800 nm via two photon absorption and probed at 7 μm; the inset shows the quadratic PIA dependence on light intensity when pumped at 800 nm.

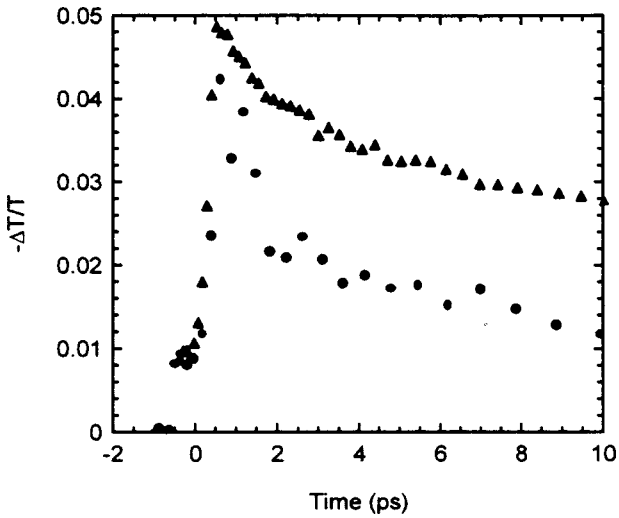

FIG. 4. Comparison of the PIA wave form in MEH-PPV (●) and MEH-PPV/C_{60} (50% C_{60}, by weight) (▲), when pumped at the same light intensity at 800 nm and probed at 7 μm.

the PIA responses in MEH-PPV and MEH-PPV/C_{60} (10% C_{60}, by weight), when pumped at 400 nm, and probed at 9 μm.

The short rise time sets an upper bound of 100 fs for the onset of the carrier generation process in PPV and MEH-PPV and for electron transfer from MEH-PPV to C_{60}.[8] Since the strengths of the IRAV mode signals are proportional to the density of carriers, these short rise times imply ultrafast carrier generation and polaron formation at times smaller by more than three orders of magnitude than the exciton lifetime ($t \sim 300$ ps).[14] Thus, any branching of the photoexcitations into the carrier and exciton channels occurs at $t < 100$ fs, most likely before the completion of the thermalization process.

The absence of correlation between the temporal behavior of the photoinduced IRAV signals from MEH-PPV (see Figs. 4 and 5) and the exciton lifetime (as determined by the decay of the photoluminescence) implies that carriers are photoexcited directly and not generated through a secondary process from exciton annihilation (e.g., from interaction with impurities, defects, etc.). Moreover, carrier generation via exciton-exciton interaction is not consistent with the linear dependence of the carrier density on light intensity.

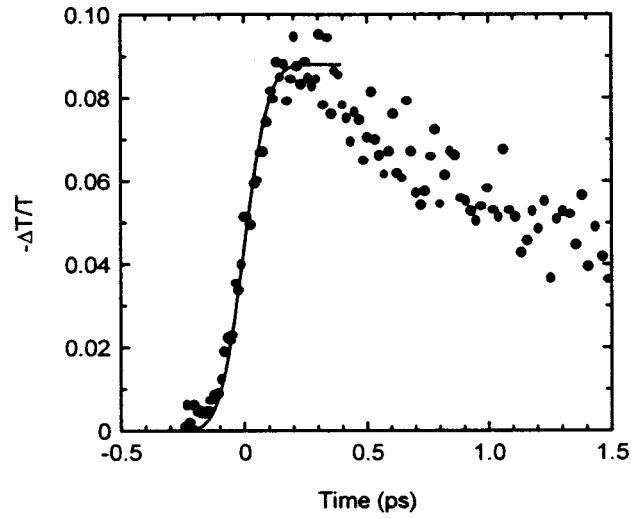

FIG. 3. Fast PIA risetime in PPV; the solid curve represents a step function convoluted with a Gaussian with 100 fs full width at half maximum.

The strength of the prompt PIA signal, PIA(0), is proportional to the charge carrier density along the probe beam path. Thus, at $t=0$; $\mathrm{PIA}(0) = -\Delta T/T \sim \sigma N_c(0) d$ for small α (relevant to pumping at 800 nm, at which the pump beam traverses the sample almost without a reduction in intensity), or $\mathrm{PIA}(0) = -\Delta T/T \sim \sigma N_c(0)/\alpha$ for large α (relevant to pumping at 400 nm), where $N_c(0)$ is the carrier density at $t=0$, σ is the cross section of the IRAV absorption bands, α is the absorption coefficient of the pump beam, and d is the sample thickness. Thus,

$$\mathrm{PIA}(0)_{\text{MEH-PPV}}/\mathrm{PIA}(0)_{\text{MEH-PPV/C}_{60}} \propto N_c(0)_{\text{MEH-PPV}}/N_c(0)_{\text{MEH-PPV/C}_{60}}. \quad (1)$$

From the data in Fig. 4, $N_c(0)_{\text{MEH-PPV}}/N_c(0)_{\text{MEH-PPV/50\% C}_{60}} = 0.3$ and from the data in Fig. 5, $N_c(0)_{\text{MEH-PPV}}/N_c(0)_{\text{MEH-PPV/10\% C}_{60}} = 0.32$. Thus, in pristine MEH-PPV, the initial charge carrier density, photogenerated in $t < 100$ fs in zero field, is smaller by only a factor of 3 than in MEH-PPV/C_{60} where the quantum efficiency approaches unity.[7,8]

To determine ϕ_0 from the measured ratio $R = N(0)_{\text{MEH-PPV}}/N(0)_{\text{MEH-PPV/C}_{60}}$, one must correct for the following: (1) The volume fraction g of MEH-PPV which was replaced by C_{60} in the MEH-PPV/C_{60} composite reduces the number of photons absorbed by the conjugated chain and thus reduces the carrier density $N(0)$; (2) The probability f of electron transfer from the polymer to C_{60} changes $N(0)$ in the MEH-PPV/C_{60} composite. Including these corrections, we obtain

$$R = 2\phi_0/\{(1-g)[\phi_0 + \phi_0(1-f) + f(1-\phi_0)]\};$$

thus,

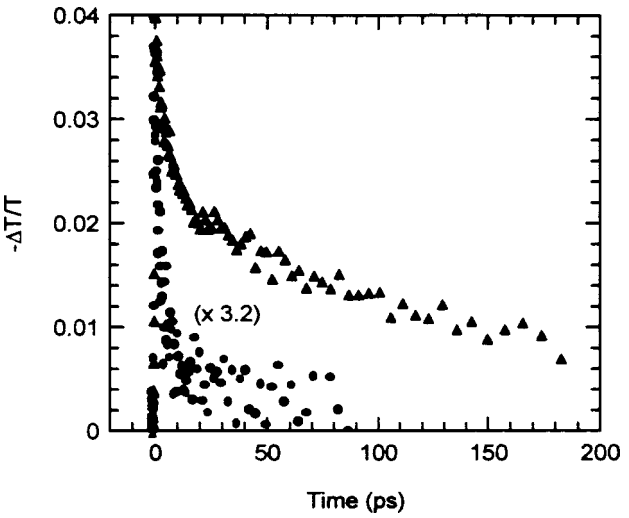

FIG. 5. Comparison of the PIA wave form in MEH-PPV (●), magnified by a factor of 3.2, and MEH-PPV/C_{60} (10% C_{60} by weight) (▲) when pumped at the same light intensity at 400 nm and probed at 9 μm.

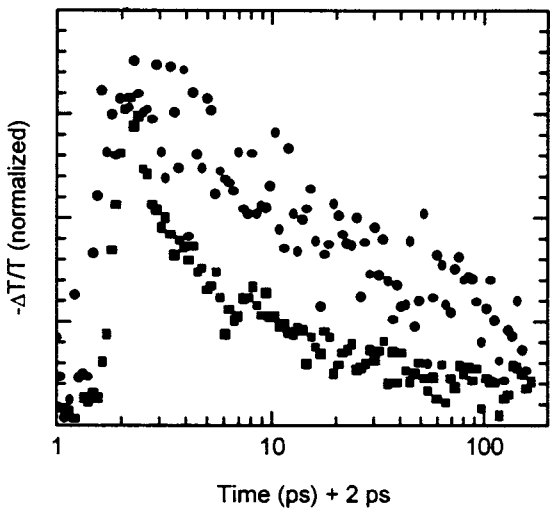

FIG. 6. The PIA signals in MEH-PP, normalized to equal light intensity, pumped at 400 nm (3.1 eV, squares) and 267 nm (4.7 eV, circles) and probed at 7 μm.

$$\phi_0 = R[(1-g)f/2]/[1-R(1-g)(1-f)]. \qquad (2)$$

Equation (2) accounts for the contribution to the PIA signal in the MEH-PPV/C_{60} composite of fraction ϕ_0 of holes directly excited along the polymer chain, the remaining fraction $\phi_0(1-f)$ electrons directly excited on the polymer chain, which in blends with a relatively small concentration of C_{60} did not undergo a charge-transfer reaction, and the fraction ($f[1-\phi_0]$) of holes left on the MEH-PPV chain following the charge-transfer reaction from excited states which do not yield free carriers. In MEH-PPV/50% C_{60}, $f \approx 1$, and $g = 0.26$. Thus, from the data in Fig. 4, $\phi_0 \approx 0.1$. For the 10% blend, $f \approx 0.5$ as inferred from the concentration dependence of the photoconductivity,[8] and $g \approx 0$ since nearly all of the 400 nm pump light is absorbed in the polymer. Thus, from the data in Fig. 5, $\phi_0 \approx 0.1$. The two values obtained from samples with different concentrations of C_{60} and using two widely different pump frequencies (one involving a direct π-π^* transition and the other involving two-photon absorption) are in agreement.

The relatively large value of ϕ_0 implies significant delocalization of the excited-state wave functions. Covalent bonding and the associated short intrachain bond lengths lead to relatively large π-electron overlap integrals and broad π and π^* bands. As a result, even in disordered films cast from solution, there is a relatively high probability that the electron-hole separation in a geminate pair will be sufficient to prevent geminate recombination.

INTERCHAIN INTERACTIONS

Comparison of the temporal evolution of the photoinduced IRAV signals in PPV (Fig. 2 and Fig. 3) and MEH-PPV (Figs. 4 and 5) reveals that the initial decay depends on the strength of the interchain interaction (there are no functional groups to separate the main chains in PPV). The $\tau \sim 250$ ps decay time obtained for oriented PPV is similar to that deduced from transient photoconductivity measurements.[15] In disordered films of MEH-PPV where the side chains reduce the interchain interaction, ϕ_0 remains large ($\phi_0 \approx 0.1$), but the photocarrier density decays within 10–15 ps (see Figs. 4 and 5). Thus, interchain hopping-tunneling enhances the spatial extent of the wave functions and reduces the probability of early time recombination. Note that ''early time'' recombination and ''geminate'' recombination are not the same; e-h pairs which undergo geminate recombination do not contribute to the current.

These observations are consistent with the photoconductivity data. The longer carrier lifetimes in PPV and MEH-PPV/C_{60} enhance the photoconductive response. The fast carrier recombination in MEH-PPV reduces the magnitude of the transient photoconductivity measured at later times ($\sim$100 ps) when most of the photocarriers have already recombined.[3,15]

DEPENDENCE OF ϕ_0 ON THE PHOTON ENERGY

In Fig. 6, we present a comparison of the PIA in MEH-PPV measured at two different pump wavelengths, 400 nm (3.1 eV, into the lowest π-π^* interband transition) and 267 nm (4.7 eV, into a higher lying excited state) and probed at 7 μm. Normalizing the data to equal pump intensity, we find that the magnitude of the ultrafast photoinduced IRAV response is insensitive to the pump photon energy; $\phi_0 \approx 0.1$ at the two photon energies. There is, however, a significantly longer carrier lifetime when pumped at 4.7 eV compared to that at 3.1 eV.

Thus, in contrast to models for the carrier generation that predict that the quantum efficiency should depend upon the photon energy (e.g., the Onsager model),[16–18] the data in Fig. 6 show that varying the pump photon energy from 3.1 to 4.7 eV does not change ϕ_0. We interpret the longer lifetime for carriers photogenerated at 4.7 eV as arising from the higher probability of interchain charge separation when the photocarriers are generated at a sufficiently high energy that the specific conjugated chain excited to a higher level acts as a ''super-donor'' to the neighboring chains. As a result, ul-

trafast interchain charge transfer is significantly enhanced at high photon energies, leading to enhanced carrier delocalization and to longer carrier lifetime. The enhanced carrier delocalization is expected to result in an increase in the carrier mobility when pumped at 267 nm as well.

The data in Fig. 6 imply a straightforward explanation for the increase in the photoconductive response above 3 eV in MEH-PPV. Since the steady-state photoconductive response is proportional to the $(\phi_0 \mu \tau)$ product, the data in Fig. 6 imply that this increase originates from the dependence of the carrier lifetime and possibly the mobility, rather than ϕ_0, on the photon energy. Such an increase of the carrier lifetime and mobility when pumped at higher photon energies is consistent with the observation that the increase in the steady-state photoconductivity above 3 eV seen in MEH-PPV persists also in MEH-PPV/50% C_{60},[2] a system for which the charge carrier QE approaches unity.

The sensitivity of the rate of recombination of carriers to the probability of interchain hopping is consistent with the larger carrier lifetime found in PPV compared to that in MEH-PPV. Thus, the onset of enhanced photoconductivity above 3 eV has a natural explanation in terms of reduced carrier recombination because of interchain charge separation.

CONCLUSION

Ultrafast photoinduced IRAV absorption measurements have enabled direct determination of the initial quantum efficiency for photogeneration of charge carriers. The data reveal photogeneration and thermalization of charged carriers and the formation of polarons, and confirm the ultrafast ($<$100 fs) electron transfer in MEH-PPV/C_{60} blends. The initial quantum efficiency for photogeneration of charged carriers in MEH-PPV, $\phi_0 \approx 0.1$, is comparable to the quantum efficiency for photoluminescence. The absence of correlation between the fast photogeneration of charge carriers ($<$100 fs) and the exciton lifetime ($\tau_{ex} \sim 300$ ps), and the linear dependence of the carrier density on pump intensity, indicate that carriers are directly photogenerated. Comparison of the recombination dynamics in MEH-PPV and PPV demonstrates the sensitivity of the initial carrier recombination processes to the magnitude of interchain interactions: higher carrier lifetime is correlated with higher probability for interchain hopping.

The quantum efficiency for carrier generation in MEH-PPV is the same ($\phi_0 \approx 0.1$) when the system is pumped either at photon energies well above the first π-π^* transition (at 267 nm, 4.7 eV) or when pumped into the first π-π^* transition (at 400 nm, 3.1 eV). The carrier lifetime, however, increases at the higher photon energy, providing a simple explanation for the increase in the photoconductivity when pumped at photon energies above 3 eV. The longer lifetime arises from interchain charge separation and indicates the important role of interchain coupling on the carrier recombination dynamics.

The relatively large quantum efficiency for photogeneration of charged carriers measured in zero applied field, the independence of the quantum efficiency on photon energy above 3 eV, the independence of the quantum efficiency on temperature, and the ultrafast photogeneration process are all inconsistent with the predictions of traditional exciton-based models of carrier generation that have been proposed for conjugated polymers (e.g., the Onsager model). The data indicate that charged carriers are primary photoexcitations.

ACKNOWLEDGMENTS

We are grateful to Professor E. W. Van Stryland and Dr. D. McBranch for providing us with the $AgGaSe_2$ crystal, and to Jian Wang for assistance with sample preparation. Dr. D. McBranch pointed out the importance of the different time scales observed for carrier decay and exciton decay. This research was supported by the Air Force Office of Scientific Research (Charles Lee, Program Officer) under F49620-99-1-0031 and by the National Science Foundation under DMR9812852.

[1] M. Chandross, S. Mazumdar, S. Jeglinski, X. Wei, Z. V. Vardeny, E. W. Kwock, and T. M. Miller, Phys. Rev. B **50**, 14 702 (1994).

[2] A. Kohler, D. A. dos Santos, D. Beljonne, Z. Shuai, J. L. Bredas, R. H. Friend, S. C. Moratti, A. B. Holmes, A. Kraus, and K. Mullen, Nature (London) **392**, 903 (1998).

[3] D. Moses, J. Wang, G. Yu, and A. J. Heeger, Phys. Rev. Lett. **80**, 2685 (1998).

[4] D. Moses, A. Dogariu, and A. J. Heeger, Chem. Phys. Lett. **316**, 356 (2000).

[5] B. Horovitz, Solid State Commun. **41**, 729 (1982).

[6] For review on the IRAV modes, see the following papers and references therein: E. Ehrenfreund and Z. V. Vardeny, Proc. SPIE **3145**, 324 (1997); Z. G. Soos, G. W. Hayden, A. Girlando, and A. Painelli, J. Chem. Phys. **100**, 7144 (1994).

[7] N. S. Sariciftci, L. Smilowitz, A. J. Heeger, and F. Wudl, Science **258**, 1474 (1992); N. S. Sariciftci and A. J. Heeger, Int. J. Mod. Phys. B **8**, 237 (1994).

[8] C. H. Lee, G. Yu, D. Moses, K. Pakbaz, C. Zhang, N. S. Sariciftci, A. J. Heeger, and F. Wudl, Phys. Rev. B **48**, 15 425 (1993); B. Kraabel, J. C. Hummelen, D. Vacar, D. Moses, and A. J. Heeger, J. Chem. Phys. **104**, 4267 (1996).

[9] W. P. Su and J. R. Schrieffer, Proc. Natl. Acad. Sci. USA **77**, 5626 (1980).

[10] U. Mizrahi, I. Shtrichman, D. Gershoni, E. Ehrenfreund, and Z. V. Vardeny, Synth. Met. **102**, 1182 (1998).

[11] C. R. Fincher, M. Ozaki, M. Tanaka, D. Peebles, L. Lauchlan, A. J. Heeger, and A. G. MacDiarmid, Phys. Rev. B **20**, 1589 (1979); K. F. Voss, C. M. Foster, L. Smilowitz, D. Mihailovic, S. Askari, G. Srdanov, Z. Ni, S. Shi, A. J. Heeger, and F. Wudl, *ibid.* **43**, 5109 (1991).

[12] M. K. Reed and M. K. Steiner-Shepard, in *Ultrafast Phenomena, X*, edited by X. P. F. Barbara, J. G. Fujimoto, W. Knox, and W. Zinth (Springer-Verlag, Berlin, 1996), p. 40.

[13] M. J. Rice and Y. N. Gartstein, Phys. Rev. B **53**, 10 764 (1996).

[14] Fast carrier photogeneration has been proposed earlier by D. Moses, in *The Nature of Photoexcitations in Conjugated Poly-*

mers, edited by N. S. Sariciftci (World Scientific, Singapore, 1997); D. Moses and A. J. Heeger, in *Relaxation in Polymers*, edited by T. Kobayashi (World Scientific, Singapore, 1993); and L. J. Rothberg, M. Yan, A. W. P. Fung, T. M. Jedju, E. W. Kwock, and M. E. Galvin, Synth. Met. **84**, 537 (1997).

[15] D. Moses, H. Okumoto, C. H. Lee, A. J. Heeger, T. Ohnishi, and T. Noguchi, Phys. Rev. B **54**, 4748 (1996).

[16] M. Pope and C. E. Swenberg, *Electronic Processes in Organic Crystals* (Oxford University Press, New York, 1982).

[17] R. C. Enck and G. Pfister, in *Photoconductivity and Related Phenomena*, edited by J. Mort and D. M. Pai (Elsevier, New York, 1976).

[18] A recent theoretical extension of the Onsager solution has been developed by H. Scher and S. Rackovsky, J. Chem. Phys. **81**, 1994 (1984).